Proceedings of the 2004 IEEE
International Conference on Robotics & Automation
New Orleans, LA • April 2004

Integrated Motion Control for Walking, Jumping and Running on a Small Bipedal Entertainment Robot

*Ken'ichiro NAGASAKA (SONY Corporation, nagasaka@erc.sony.co.jp)†
Yoshihiro KUROKI (SONY Corporation, kuroki@erc.sony.co.jp)†
Shin'ya SUZUKI (SONY Corporation, ssuzuki@erc.sony.co.jp)†
Yoshihiro ITOH (SONY Corporation, yitoh@erc.sony.co.jp)†
Jin'ichi YAMAGUCHI (Tama Research Institute, yamajin@erc.sony.co.jp)‡
†5-11-3 Shimbashi, Minato-ku, Tokyo 105-0004 Japan
‡5-14-38 Tamadaira, Hino-shi, Tokyo 191-0062 Japan

Abstract— **This paper proposes the integrated motion control method to make a bipedal humanoid walk, jump and run. This method generates dynamically consistent motion patterns in real-time based on the concept of dynamics filter, which assures that the force and the moment generated by the robot can equilibrate with those acted by the environment. The validity of the algorithm is verified by the dynamic simulation. The proposed method is applied to the real humanoid "QRIO" under the adaptive control, and the stable walking, jumping and running including the transitions between them are realized.**

I. Introduction

A humanoid robot, which has a human-like form and behaves like a human being autonomously, presents unique characteristics that can not be found in the previous products and is beginning to create the new values in the field of art and entertainment. QRIO project has been working on exploiting such a new field of robotics from the two key points of view; "motion entertainment" and "communication entertainment" [1][2][3].

The current motion control for QRIO is based on the ability of stable and flexible biped walking by "Real-time Integrated Adaptive Motion Control[3]". However it will be desired that a humanoid robot can perform not only the motion which always keeps in contact with the ground like walking but also the motion which includes flight phases like jumping or running so as to advance into the new entertainment field like a sport game by humanoid robots using more dynamic and rapid motions.

Matsuoka[4] and Raibert [5] have dealt with the balance control for the bipedal hopping robot in 1980s. However, these methods can be hardly applied to practical use because they assumes the leg with no mass, which imposes strong restrictions on the mechanical design. On the other hand, the control method for biped walking using ZMP stability criterion [6][7] is widely adopted as the practical method by the many humanoids since it's almost free from this kind of restrictions. So recently the several control methods that generate motion patterns (positional references) for jumping and running are proposed [8] [9] [10], which can be applied to the mechanical systems that are designed to walk based on the ZMP.

Furthermore, there are some other important requirements for the design of the controller for running or jumping. First, the transitions between walking, jumping, running and standing state must be taken into account. The controller which can only cope with each stationary state will be insufficient. Secondly, the flexibility to satisfy the run-time various requests for the change of the gait pattern will be important. The gait parameters like step lengths, step cycles and rotation angles can be changed by the client processes at any time. The off-line pattern generation will be inappropriate.

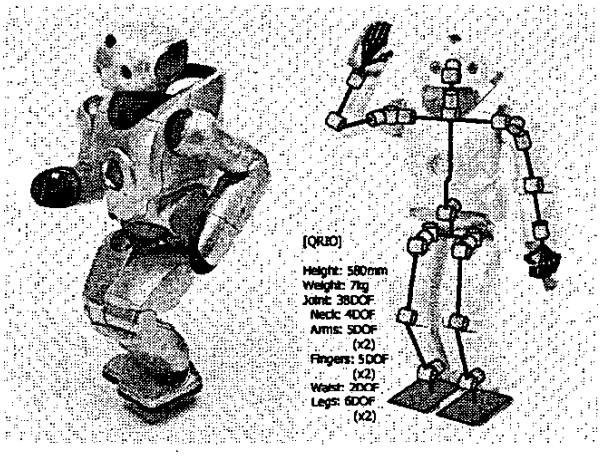

Fig. 1. QRIO's appearance and configuration

This paper presents the integrated motion control method for biped walking, jumping and running to satisfy these requirements. It's based on a kind of the concept of dynamics filter [8] [11], which generates motion patterns in real time so that the force and the moment generated by the robot can equilibrate with the force and the moment acted by the environment. The basic concept of the dynamics filter is explained in section II. In section III, the configuration of QRIO is shown. In section IV, the mathematical model is derived. The validity of the algorithm is verified by the dynamic simulation in section V. Is is applied to the real humanoid "QRIO" under the adaptive control in section VI. Finally we summarize in section VII.

0-7803-8232-3/04/$17.00 ©2004 IEEE

TABLE I

QRIO'S BASIC SPECIFICATION

CPU	64bit RISC Processor (× 3)
Memory	64MB DRAM (× 3)
OS / Architecture	Aperios / Open-R
Program Supplying Media	16MB Memory Stick
I/F	PC Card Slot, MS Slot
CCD	110,000 pixels 1/5 inch CCD
Sound	7 Microphes, Speaker
Weight	7.0kg
Dimensions (H/W/D)	580 × 260 × 190[mm]

II. Dynamic Constraints in Stance and Flight Phases

The motion pattern for a legged robot can't be performed as planned unless it is designed under the consideration of the dynamics. Generally, a robot follows the designed motion trajectory only when it is designed so that the force $\boldsymbol{f}$ and the moment $\boldsymbol{n}$ required to support the motion can be gotten from the environment as a counteraction. That is, we must impose a constraint condition on $\boldsymbol{f}$ and $\boldsymbol{n}$ so that there exists a combination of an external force $\boldsymbol{F}$ and an external moment $\boldsymbol{N}$ that satisfies $\boldsymbol{F} = \boldsymbol{f}$ and $\boldsymbol{N} = \boldsymbol{n}$. We call the constraint conditions of this kind concerning the dynamic equilibrium condition "dynamic constraints".

It is known that the dynamic constraint while the robot is on the ground is equivalent to the condition that the vertical reaction force is upward besides ZMP is within the support polygon. That is,

$$f_z > 0 \ \wedge \ M_x = 0 \ \wedge \ M_y = 0 \tag{1}$$

where $\boldsymbol{M}$ is the moment around a point $\boldsymbol{p}$ within the support polygon. On the other hand, while the robot is off the ground, the external force/moment except the gravity force can't be applied by the environment. So,

$$\boldsymbol{f} = -m\boldsymbol{g} \ \wedge \ \boldsymbol{n} = \boldsymbol{0} \tag{2}$$

gives the dynamic constraint. Here m is a total mass of the robot. Our proposed method realizes the flexible and swift transitions between walking, jumping and running by repeating the process to generate the whole body motion pattern for a certain period in real-time so that it satisfies eq.(1) in stance phases and eq.(2) in flight phases.

III. Configuration of QRIO

QRIO's apperance and configuration are shown in Fig.1. QRIO has the height of 580[mm] and the weight of 7[kg] including the CPU and the battery. Its moving parts consists of totally 38 degrees of freedom, and each joint (except the joints in the hands and the neck) is driven by the actuator unit called ISA (Intelligent Servo Actuator) which has a motor driver and communication circuits build-in. The actuators carry out the positional servo according to the positional reference value sent from the host CPU via the serial communication based on the Open-R bus protocol. For this research, both of the torque and the rotational speed of ISA were raised by about 20%.

QRIO has 3-axes accelerometers and gyroscopic sensors in the pelvis part, 2-axes accelerometers and four force sensors in each foot. Contact sensors are distributed on the head, the shoulder, the hands, the grip in the neck, the thigh, the knee, the shank, the ankle, the armpit, the elbow and so on. They are used for non-verbal communication and safety control. The stereo vision system using CCD cameras and 7 microphones are mounted in the head part, which are used for environment recognition, sound source localization, speaker recognition, speech recognition and others. The basic specification of QRIO is shown in Table.I.

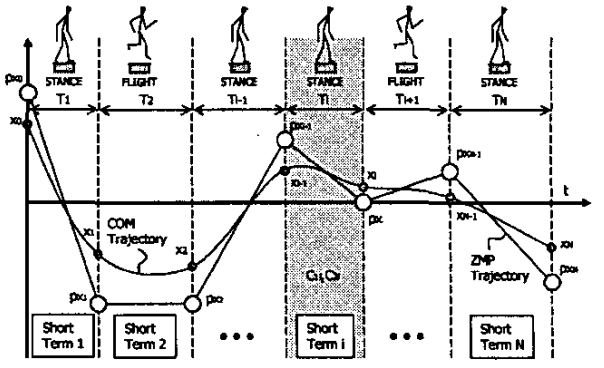

Fig. 2. Division of a motion into short linear periods

IV. Control Scheme

In this section, the mathematical model to calculate the whole body motion pattern in real-time so as to satisfy the dynamic constraints described in the section II is derived.

A. Constraints on the horizontal COM trajectory

In a stance phase, let $\boldsymbol{x} = (x, y, z)^T$ be the position of the COM (Center Of Mass) of the robot, then the dynamic constraint of eq.(1) concerning the moment is expressed as the following equation:

$$\boldsymbol{M} = (\boldsymbol{x} - \boldsymbol{p}) \times m(\ddot{\boldsymbol{x}} + \boldsymbol{g}) + \boldsymbol{n} = \begin{bmatrix} 0 \\ 0 \\ * \end{bmatrix} \tag{3}$$

As the moment around ZMP is mainly caused by the movement of the COM in most cases, the second term of eq.(3) can be neglected for simplicity (although it can be estimated using inverse dynamics if precision is required). The the x and y elements are expressed as,

$$\begin{aligned} (z - p_z)\ddot{x} - (x - p_x)(\ddot{z} + g) &= 0 \\ (z - p_z)\ddot{y} - (y - p_y)(\ddot{z} + g) &= 0 \end{aligned} \tag{4}$$

To get the analytical solution without difficulty, the relatively short period of $T[sec]$ is introduced here. In such a short term, the following approximations will be valid.

- ZMP trajectory has no acceleration.
- The height of COM is constant.

The boundary values of the analytical solution gotten on these assumptions are,

$$\begin{aligned} x(0) &= p_x(0) + C_1 + C_2 \\ \dot{x}(0) &= \dot{p}_x(0) + \lambda(C_1 - C_2) \\ x(T) &= p_x(T) + C_1 e^{\lambda T} + C_2 e^{-\lambda T} \\ \dot{x}(T) &= \dot{p}_x(T) + \lambda\left(C_1 e^{\lambda T} - C_2 e^{-\lambda T}\right) \end{aligned} \tag{5}$$

where C_1, C_2 are undetermined coefficients and $\lambda = \sqrt{g/(z-p_z)}$. For convenience only the elements concerning x direction are shown. The general motion can be thought to consist of N short terms as shown in the Fig.2. Let T_i be the duration, C_{1_i} and C_{2_i} be the undetermined coefficients, λ_i be the eigenvalue, p_{x_i} be the terminal value of the ZMP of the i-th short term respectively, then the boundary values of the analytical solution in the i-th short term can be generally expressed as follows.

$$\begin{aligned} x_{i-1} &= p_{x_{i-1}} + C_{1_i} + C_{2_i} \\ \dot{x}_{i-1} &= \dot{p}_{x_{i-1}} + \lambda_i (C_{1_i} - C_{2_i}) \\ x_i &= p_{x_i} + C_{1_i} e^{\lambda_i T_i} + C_{2_i} e^{-\lambda_i T_i} \\ \dot{x}_i &= \dot{p}_{x_i} + \lambda_i \left(C_{1_i} e^{\lambda_i T_i} - C_{2_i} e^{-\lambda_i T_i}\right) \end{aligned} \tag{6}$$

Similarly we can define the same kind of short terms in a flight phase. As the external forces can't be applied in the horizontal direction there because of eq.(2), we can get

$$m\ddot{x} = 0 \tag{7}$$

, where only the element concerning x-direction is written for convenience. The boundary values of the analytical solution in the i-th short term are,

$$\begin{aligned} x_{i-1} &= C_{1_i} \\ \dot{x}_{i-1} &= C_{2_i} \\ x_i &= C_{1_i} + C_{2_i} T_i \\ \dot{x}_i &= C_{2_i} \end{aligned} \tag{8}$$

The general motions can be modelled as the combination of these short periods of stance or flight phases. Under this modelling concept, the undetermined coefficients C_{1_i} and C_{2_i} are determined so that the position and the velocity of COM become continuous at the boundaries of each short period. The continuity condition about the position and the velocity of COM at the boundary between the i-th term ($\mathcal{ST}_i$) and its preceding term ($\mathcal{ST}_{i-1}$) can be divided into the following four cases according to whether the adjacent two short terms belong to a stance phase or a flight phase, respectively.

- $\mathcal{ST}_{i-1} \in$ *stance* and $\mathcal{ST}_i \in$ *stance* :
  Referring to eq.(6), we can get the continuity condition about x_i and $\dot{x}_i$ at the boundary between $\mathcal{ST}_{i-1}$ and $\mathcal{ST}_i$ as,

$$\begin{aligned} &C_{1_i} + C_{2_i} = C_{1_{i-1}} e^{\lambda_{i-1} T_{i-1}} + C_{2_{i-1}} e^{-\lambda_{i-1} T_{i-1}} \\ &\tfrac{p_{x_i} - p_{x_{i-1}}}{T_i} + \lambda_i (C_{1_i} - C_{2_i}) = \tfrac{p_{x_{i-1}} - p_{x_{i-2}}}{T_{i-1}} \\ &\quad + \lambda_{i-1} \left(C_{1_{i-1}} e^{\lambda_{i-1} T_{i-1}} - C_{2_{i-1}} e^{-\lambda_{i-1} T_{i-1}}\right) \end{aligned} \tag{9}$$

- $\mathcal{ST}_{i-1} \in$ *flight* and $\mathcal{ST}_i \in$ *stance* :
  Referring to eq.(8) and eq.(6), we can get the continuity condition about x_i and $\dot{x}_i$ at the boundary between $\mathcal{ST}_{i-1}$ and $\mathcal{ST}_i$ as,

$$\begin{aligned} &p_{x_{i-1}} + C_{1_i} + C_{2_i} = C_{1_{i-1}} + C_{2_{i-1}} T_{i-1} \\ &\tfrac{p_{x_i} - p_{x_{i-1}}}{T_i} + \lambda_i (C_{1_i} - C_{2_i}) = C_{2_{i-1}} \end{aligned} \tag{10}$$

- $\mathcal{ST}_{i-1} \in$ *stance* and $\mathcal{ST}_i \in$ *flight* :
  Referring to eq.(6)and eq.(8), we can get the continuity condition about x_i and $\dot{x}_i$ at the boundary between $\mathcal{ST}_{i-1}$ and $\mathcal{ST}_i$ as,

$$\begin{aligned} &C_{1_i} = p_{x_{i-1}} + C_{1_{i-1}} e^{\lambda_{i-1} T_{i-1}} + C_{2_{i-1}} e^{-\lambda_{i-1} T_{i-1}} \\ &C_{2_i} = \tfrac{p_{x_{i-1}} - p_{x_{i-2}}}{T_{i-1}} \\ &\quad + \lambda_{i-1} \left(C_{1_{i-1}} e^{\lambda_{i-1} T_{i-1}} - C_{2_{i-1}} e^{-\lambda_{i-1} T_{i-1}}\right) \end{aligned} \tag{11}$$

- $\mathcal{ST}_{i-1} \in$ *flight* and $\mathcal{ST}_i \in$ *flight* :
  Referring to eq.(8), we can get the continuity condition about x_i and $\dot{x}_i$ at the boundary between $\mathcal{ST}_{i-1}$ and $\mathcal{ST}_i$ as,

$$\begin{aligned} C_{1_i} &= C_{1_{i-1}} + C_{2_{i-1}} T_{i-1} \\ C_{2_i} &= C_{2_{i-1}} \end{aligned} \tag{12}$$

The continuity conditions about the position and the velocity of COM at the boundaries of the short terms must be established concerning $i = 2..N$.

In the beginning of the motion, the boundary conditions are imposed so as to satisfy the given COM position $\bar{x}_0$ and its velocity $\dot{\bar{x}}_0$. The initial boundary conditions can be divided into the following two cases according to whether the initial short term ($\mathcal{ST}_1$) belongs to a stance phase or a flight phase.

- $\mathcal{ST}_1 \in$ *stance* :
  Referring to eq.(6), we can get the initial boundary condition in the 1st short term as,

$$\begin{aligned} &C_{1_1} + C_{2_1} + p_{x_0} = \bar{x}_0 \\ &\tfrac{p_{x_1} - p_{x_0}}{T_1} + \lambda_1 (C_{1_1} - C_{2_1}) = \dot{\bar{x}}_0 \end{aligned} \tag{13}$$

- $\mathcal{ST}_1 \in$ *flight* :
  Referring to eq.(8), we can get the initial boundary condition in the 1st short term as,

$$\begin{aligned} C_{1_1} &= \bar{x}_0 \\ C_{2_1} &= \dot{\bar{x}}_0 \end{aligned} \tag{14}$$

Similarly, in the terminal period $\mathcal{ST}_N$, the boundary conditions are imposed so as to satisfy the given COM position $\bar{x}_N$ and its velocity $\dot{\bar{x}}_N$. The terminal boundary conditions can be also divided into the following two cases according to whether the terminal short term $\mathcal{ST}_N$ belongs to a stance phase or a flight phase.

- $\mathcal{ST}_N \in$ *stance* :
  Referring to eq.(6), we can get the terminal boundary condition in the N-th short term as,

$$\begin{aligned} &p_{x_N} + C_{1_N} e^{\lambda_N T_N} + C_{2_N} e^{-\lambda_N T_N} = \bar{x}_N \\ &\tfrac{p_{x_N} - p_{x_{N-1}}}{T_N} + \lambda_N \left(C_{1_N} e^{\lambda_N T_N} - C_{2_N} e^{-\lambda_N T_N}\right) = \dot{\bar{x}}_N \end{aligned} \tag{15}$$

- $\mathcal{ST}_N \in$ *flight* :
  Referring to eq.(8), we can get the terminal boundary condition in the N-th short term as,

$$\begin{aligned} C_{1_N} + C_{2_N} T_N &= \bar{x}_N \\ C_{2_1} &= \dot{\bar{x}}_N \end{aligned} \tag{16}$$

The position and the velocity of COM in the previous control cycle are substituted for the initial values, $\bar{x}_0$ and $\dot{\bar{x}}_0$, respectively to get the COM trajectory that connects with the current motion state smoothly. The middle point of the both feet after few steps can be used for $\bar{x}_N$ in the terminal condition. Zero can be substituted for $\dot{\bar{x}}_N$. This is just one instance of settings, which constrains the motion of COM to converge above the middle point of the both feet after few steps. In the real-time motion pattern generation, we have only to ensure the stability during the relatively short duration until the next calculation, so this kind of rough convergence conditions can be used.

The boundary of each short terms is set as the boundary between a double support phase and a single support

phase, or the boundary between a stance phase and a flight phase, for instance. The equations of eq.(9)..eq.(16) give $2N+2$ constraints. Therefore, more than two variables must be added in addition to $2N$ undetermined coefficients $C_{1_i}, C_{2_i} (i = 1..N)$. Here, we use the positions of ZMP $p_{x_i} (i = 1..N)$ as these additional variables. This problem will be treated as the optimization problem because the number of the variables are redundant in general. For example, we can solve it as the following quadratic programming problem that minimizes the sum of the square of the difference between the preset ZMP $\bar{p}_{x_i} (i = 1..N)$ and $p_{x_i} (i = 1..N)$ subject to the equational constraints from eq.(9) to eq.(16).

$$\min \sum (\bar{p}_{x_i} - p_{x_i})^2 \tag{17}$$

The equations from eq.(9) to eq.(16) can be solved also as the simple $2N+2$ simultaneous equations by adding only two variables, p_{x_j} and p_{x_k}. In any case, once the values of these variables are determined, the horizontal position of COM satisfying the dynamic constraints in both of stance and flight phases can be calculated at any time.

B. Constraints on the vertical COM trajectory

Although the trajectory required by users are used as the default vertical trajectory of COM, it is modified to satisfy the dynamic constraints based on the z element of eq.(2) ($f_z = -mg$) in a flight phase. That is,

$$m\ddot{z} = -mg \tag{18}$$

Its analytical solution is

$$\begin{aligned} z &= -\tfrac{1}{2}gt^2 + \left(\tfrac{z_2 - z_1}{T} + \tfrac{1}{2}gT\right)t + z_1 \\ \dot{z} &= -gt + \left(\tfrac{z_2 - z_1}{T} + \tfrac{1}{2}gT\right) \end{aligned} \tag{19}$$

, where T is the duration of flight, z_1 and z_2 are the heights of COM at the moment of leaving and landing on the ground respectively. The vertical trajectory of COM in a flight phase are substituted for this parabola. On the other hand, no severe dynamic constraint is imposed on it in a stance phase as long as it satisfies $f_z > 0$. So it is only modified by the appropriate curve that satisfies $f_z > 0$ so as to connect with the parabola, eq.(19), smoothly.

C. Constraints on angular momentum

Here the rest of the dynamic constraints concerning the moment in eq.(2) during a flight phase is taken into account. Let $\boldsymbol{L}$ be the angular momentum around COM, then the equation of motion concerning the rotational motion of the robot can be expressed as follows:

$$\frac{d}{dt}\boldsymbol{L} = \boldsymbol{n} \tag{20}$$

Substitute $\boldsymbol{n} = \boldsymbol{0}$ of eq.(2) and integrate eq.(20), then we get

$$\boldsymbol{L} = \bar{\boldsymbol{L}} = const \tag{21}$$

This tells us that the constraint to keep the angular momentum constant, $\bar{\boldsymbol{L}}$, is imposed in a flight phase. The value of $\bar{\boldsymbol{L}}$ can be determined by users. The simplest way will be $\bar{\boldsymbol{L}} = \boldsymbol{0}$, but it's not the only one.

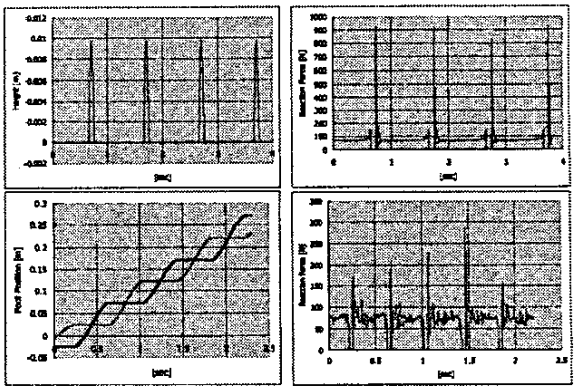

Fig. 3. Foot trajectories and vertical reaction forces in the simulation

D. Decomposition to joint angles

Lastly the infinitesimal changes in the joint angles are calculated using Jacobian so as to satisfy all the constraint conditions concerning the position of COM and the angular momentum mentioned above. Let $\boldsymbol{p_b}$, $\boldsymbol{\alpha_b}$ and $\boldsymbol{\theta}$ be the position of pelvis, its orientation (e.g. Euler angle) and the joint angles respectively, the state vector of the robot can be expressed as the concatenated vector $\boldsymbol{q} = \left[\boldsymbol{p_b}^T \boldsymbol{\alpha_b}^T \boldsymbol{\theta}^T\right]^T$.

The velocity of COM $\dot{\boldsymbol{x}}$, can be related to the state vector by the equation, $\dot{\boldsymbol{x}} = \boldsymbol{J_x}\dot{\boldsymbol{q}}$[12]. In the same manner, the angular momentum $\boldsymbol{L}$, the velocity of the i-th link $\dot{\boldsymbol{p}}_i$ and its angular velocity $\dot{\boldsymbol{\omega}}_i$ are expressed as $\dot{\boldsymbol{L}} = \boldsymbol{J_L}\dot{\boldsymbol{q}}$, $\dot{\boldsymbol{p}}_i = \boldsymbol{J}_{\boldsymbol{p}_i}\dot{\boldsymbol{q}}$ and $\dot{\boldsymbol{\omega}}_i = \boldsymbol{J}_{\boldsymbol{\omega}_i}\dot{\boldsymbol{q}}$ respectively, where $\boldsymbol{J}_*$ indicates a Jacobian.

The various constraints can be imposed on the position of COM, the angular momentum and the position/orientation of the link using these relations. These constraints can be put together and be solved as the following simultaneous equation.

$$\boldsymbol{v} = \boldsymbol{J}\dot{\boldsymbol{q}} \tag{22}$$

, where $\boldsymbol{v}$ is a vertically concatenated vector of the constrained physical quantities and $\boldsymbol{J}$ is a matrix made up by arranging the above Jacobians vertically. The state velocity $\dot{\boldsymbol{q}}$ gotten as its solution can be numerically integrated to get the state vector in the next control cycle.

In this paper, as the simplest case, the joint angles in lower limbs and the position/orientation of the pelvis are treated as the variables subject to the constraints on COM, the angular momentum, the position/orientation of each foot and the joint angles in the upper body. However the constraint on the angular momentum is released and the orientation of the pelvis is eliminated from the variables during a stance phase. Instead, the default trajectory modified to connect with the flight phase smoothly is applied to the orientation of the pelvis.

V. Dynamics Simulation

The proposed control method was verified on the dynamics simulation. We've also developed the real-time trajectory generator of the foot position/orientation and ZMP for walking, jumping and running. The combination

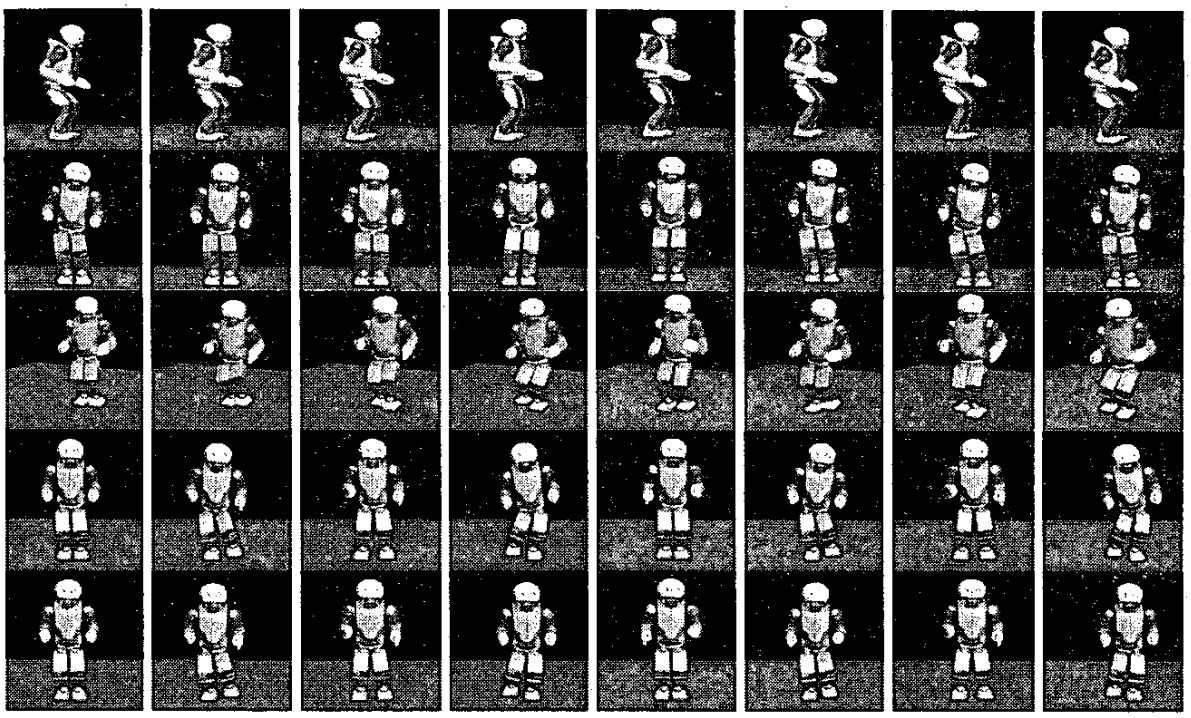

Fig. 4. Snapshots of the simulation (time passes rightward)

of the control method and the trajectory generator enables flexible transitions between these motions.

Fig.3 shows the results of the simulation done to verify the validity of the proposed control method. The simulation was carried out under the condition of the rigid floor and the high gain positional servo to keep the consistency with the theoretical model. The upper figures show the height of the foot (left figure) and the total vertical reaction force (right figure) in jumping at the same place, where the cycle is 1[s], the maximum foot height is 0.01[m] and the duration of flight is 0.1[s]. The lower figures show the horizontal position of each foot (left figure) and the total vertical reaction force (right figure) in running, where the step length is 0.05[m], the cycle is 0.4[s] and the duration of flight is 0.04[s]. In any case, the designed trajectories and the flight durations are almost realized, which reveals the validity of the proposed method.

Fig.4 shows some snapshots of the simulation. The first row shows jumping forward, the second shows jumping leftward, the third shows running forward and the fourth shows running leftward. In these examples all the dynamic constraints of eq.(1) and eq.(2) are taken into account. However, the operation of the orientation of the pelvis often causes some load concentrations and self interferences in the hip joint. On the other hand, the example of the fifth row shows running leftward, where the pelvis orientation is not operated because the momentum compensation around COM is disabled. Here the error of the moment exists, so the adaptive control which is the extended version of "Real-time Integrated Adaptive Motion Control" to do with both of stance and flight phases is applied. In most cases, such an abridged controller that satisfies

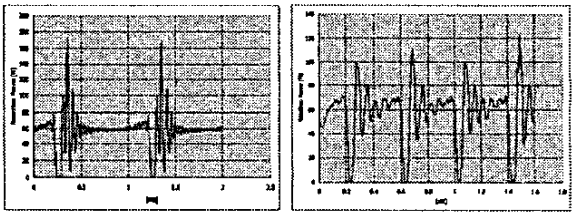

Fig. 5. Vertical reaction forces in jumping (left figure) and running (right figure) on QRIO

only a part of the dynamic constraints will be sufficient to perform stable walking, jumping and running because the duration of flight is short. It is thought to be useful from the view of motion entertainment because the pelvis orientation can be used to choreograph.

VI. Experiments on QRIO

The proposed method was applied to QRIO on which CPUs and the battery are loaded. Differing from the theoretical model, there are some limitations of torque and rotational velocity in each actuator on the real robot. To absorb this modelling error, the adaptive control is applied, which is the extended version of "Real-time Integrated Adaptive Motion Control" to do with both of stance and flight phases. Under this condition, the stable walking, jumping and running including the transitions between them were realized.

Fig.5 shows the total vertical reaction force measured by the force sensors during jumping (left figure) and running

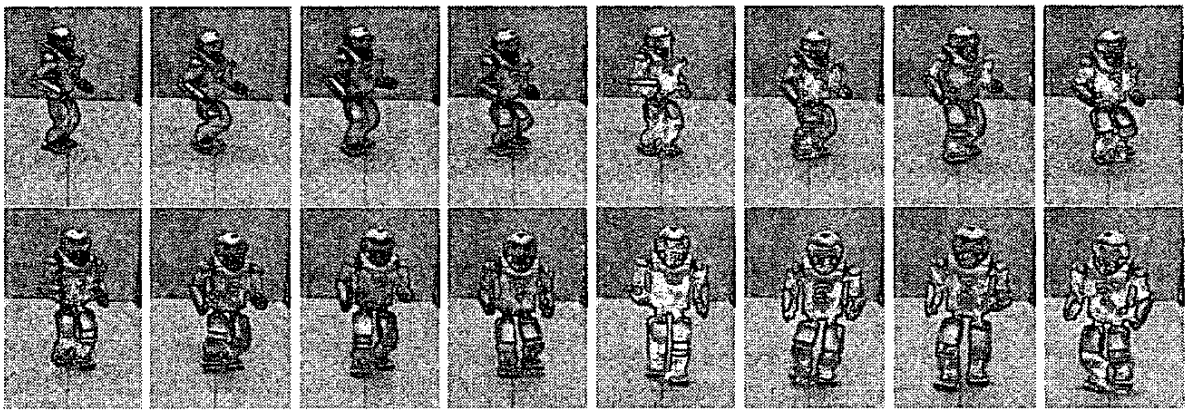

Fig. 6. Snapshots of the runnning experiment on the real robot (time passes rightward)

(right figure), where the gait parameters like the cycle and the duration of flight are same as in the simulation. In any case, there's the period of $F_z = 0$, so the flight was realized. However its duration is about 40% of the designed value because of the limitations of the real devices as mentioned above.

Fig.6 shows the snapshots of running along the curve. In this example, the momentum compensation around COM is disabled, so the pelvis orientation is not operated. The stable walking, jumping and running can be performed under the adaptive control even if such a abridged motion pattern generator that satisfies only a part of the dynamic constraints is applied, which is the same result as in the simulation.

VII. Conclusion

In this paper, the integrated motion control method for biped walking, jumping and running was described, which is based on a kind of concept of dynamics filter that generates dynamically consistent motion patterns in real time. It is a generalized concept of the control method using the ZMP stability criterion, and can be widely used for the robot driven by the positional servo control.

The validity of this method was verified using a dynamics simulation, where the foot trajectories and the duration of the flight phase were almost realized as designed. In addition, the simplified motion pattern generator that satisfies only a part of the dynamic constraints was applied under the adequate adaptive control. It can also keep stable jumping and running, which would be useful for the robot whose CPU resource is restricted.

On the other hand, the duration of flight tends to be less than the planned value. Although this degradation is mainly caused by the limitation of the actuator's capability, it will be improved by cooperating the redundant joints to avoid the concentration of the load on the specific joint.

Acknowledgment

The authors would like to thank Dr. T.Doi, the head manager of the former Intelligent Dynamics Laboratory, and all the persons concerned in QRIO's development for supporting this research.

References

[1] Y.Kuroki, T.Ishida, J.Yamaguchi, M.Fujita and T.Doi, "A Small Biped Entertainment Robot", Proc. of the IEEE-RAS International Conference on Humanoid Robots, pp.181-186, 2001.

[2] Y.Kuroki, T.Fukushima, K.Nagasaka, T.Moridaira, T.Doi, J.Yamaguchi, "A Small Biped Entertainment Robot Exploring Human-Robot Interactive Applications", Proc. of the 2003 IEEE Workshop Robot and Human Interactive Communication, pp.303-308, 2003.

[3] Y.Kuroki, M.Fujita, T.Ishida, K.Nagasaka and J.Yamaguchi, "A Small Biped Entertainment Robot Exploring Attractive Applications", Proc. of the 2003 IEEE International Conference on Robotics and Automation, pp.471-476, 2003.

[4] K.Matsuoka, "A Mechanical Model of Repetitive Hopping Movements", Biomechanisms 5, pp.251-258, 1980.

[5] M.H.Raibert, Jr.H.B.Brown and M.Chepponis, "Experiments in Balance with a 3D One-Legged Hopping Machine", In the International Journal of Robotics Research Vol.3 No.2, pp.75-92, 1984.

[6] J.Yamaguchi, E.Soga, S.Inoue and A.Takanishi, "Developoment of a Bipedal Humanoid Robot - Control Method of Whole Body Cooperative Dynamic Biped Walking-", Proc. of the 1999 IEEE International Conference on Robotics and Research, pp.368-374, 1999.

[7] K.Nagasaka, H.Inoue and M.Inaba, "Dynamic Walking Pattern Generation for a Humanoid Robot Based on Optimal Gradient Method", Proc. of the 1999 IEEE Systems, Man, and Cybernetics Conference, pp. VI908-VI913, 1999.

[8] K.Nagasaka, "The Whole-body Motion Generation for a Humanoid Robot Based on the Dyanmics Filter (Japanese)", PhD Thesis, Univ. Tokyo, 2000.

[9] T.Sugihara, and Y.Nakamura, "Variable Impedant Inverted Pendulum Model Control for a Seamless Contact Phase Transition on Humanoid Robot", Proc. of International Conference on Humanoid Robots, 5b-06, 2003.

[10] T.Nagasaki, S.Kajita, K.Yokoi, K.Kaneko and K.Tanie, "Running Pattern Generation and Its Evaluation Using a Realistic Humanoid Model", Proc. of the 2003 IEEE International Conference on Robotics and Research, pp.1336-1342, 2003.

[11] K.Yamane and Y.Nakamura, "Dynamics Filter -Concept and Implementation of On-Line Motion Gen-erator for Human Figures", Proc. of the 2000 IEEE International Conference on Robotics and Research, pp.688-695, 2000.

[12] R. Boulic, R. Mas and D. Thalmann, "Position Control of the Center of Mass for Articulated Figures in Multiple Support", Proc. of the 6th Eurographics Workshop on Animation and Simulation, pp.130-143, 1995.